RESEARCH ARTICLE | APRIL 03 2025

Simulation of turbulent flow around a thin rectangle using k-ε turbulence and environment models comsol multiphysics

Muzaffar Hamdamov ✉; Sardorbek Muzaffarov

AIP Conf. Proc. 3265, 060013 (2025)
https://doi.org/10.1063/5.0265168

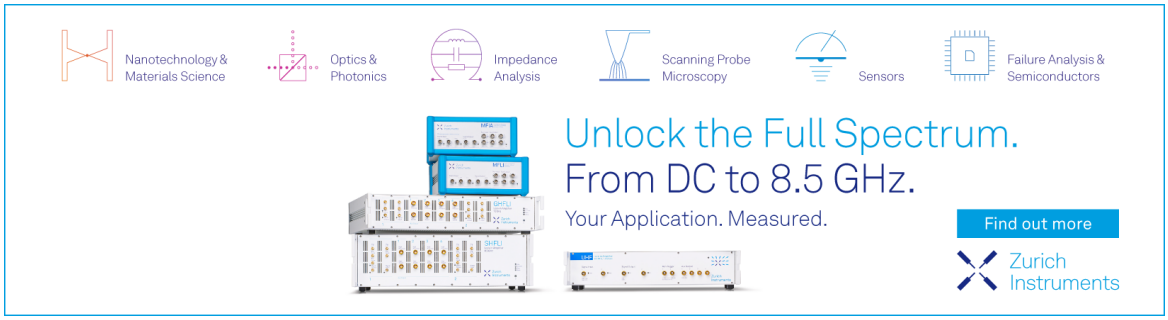

Simulation of Turbulent Flow Around a Thin Rectangle Using k-ε Turbulence and Environment Models Comsol Multiphysics

Muzaffar Hamdamov[1, a)] and Sardorbek Muzaffarov[1, b)]

[1]*Institute of Mechanics and Seismic Stability of Structures named after M.T. Urazbaev, Uzbekistan Academy of Sciences, Tashkent, Uzbekistan*

[a)] Corresponding author: mmhamdamov@mail.ru
[b)] muzaffarovs9@gmail.com

Abstract. This article presents the results of a study of the aerodynamics of a vertical - axis wind turbine blade by numerically solving the Reynolds-averaged Navier-Stokes equations and using the finite volume method. Some results of calculating the flow around a rectangular airfoil using standard Comsol solvers are presented. Multiphysics with in $k-\varepsilon$ turbulence models at Reynolds numbers 10 000<Re<2 000 0000 and angle of attack α=0°–20°. Speed results were obtained for different angle values.

INTRODUCTION

Recently, various measures have been taken in the fuel and energy industry of Uzbekistan aimed at further increasing the efficiency of energy use both in industry and at home, as well as introducing more economical technologies for the use of electricity and renewable energy sources.

Solar, hydraulic, wind, geothermal and biomass energy are the main components of Uzbekistan's renewable energy sources. The research results showed that the technical potential of the Republic of Uzbekistan for the use of renewable energy sources is 180 million tons of oil equivalent, which is more than three times its annual energy demand.

Uzbekistan has begun to widely use non-traditional and renewable energy sources. The use of wind energy is one of their main types, which is environmentally friendly and affordable.

By 2030, Uzbekistan plans to produce a quarter of its electricity from renewable energy sources. To attract private capital, the country's government offers a wide range of benefits, including long-term guarantees for the purchase of green energy. In addition, Uzbekistan works with Chinese and other leading companies for the production and installation of solar and wind panels.

The large power industry mainly uses horizontal axis wind turbines. But in populated areas and small industrial facilities remote from the power supply network, vertical axis wind turbines can be used. They have a simpler design than horizontal axis machines, and their lower blade speeds reduce safety and noise concerns. Although vertical axis turbines do offer significant operational advantages, development has been hampered by the difficulty of modeling the aerodynamics involved as well as their rotating geometry [1]. Torque is transmitted by the shaft from the blades to the generator. Like ancient sailing ships, the aerodynamic power of a modern wind turbine is based on lift rather than drag.

Two rectangular orifice wing models were designed and tested in the Duke University wind tunnel to better understand the effects of damage [2]. A rectangular hole is used to simulate damage. A wing with a hole is structurally modeled with a thin elastic plate using the finite element method. The unsteady aerodynamics of a plate wing with an opening is modeled using the doublet lattice method. The equations of aeroelastic motion are derived using the Lagrange equation. The flutter boundary is found using the Vg method. The location of the opening affects the mass, stiffness, aerodynamics and therefore the aeroelastic properties of the wing. It is shown that linear theoretical models are capable of predicting critical flutter speed and frequency, confirmed by wind tunnel tests.

International Conference: "Ensuring Seismic Safety and Seismic Stability of Buildings and Structures, Applied Problems of Mechanics"
AIP Conf. Proc. 3265, 060013-1–060013-7; https://doi.org/10.1063/5.0265168
Published under an exclusive license by AIP Publishing. 978-0-7354-5160-5/$30.00

Turbulent separated flows are an important part of modern aerodynamics due to the need to analyze non-standard flight conditions and solve other problems inextricably linked with the phenomenon of flow separation from a streamlined surface [3–5]. It is now known that numerical simulations of separated flows can be performed using various turbulence models and even an ideal fluid model, where numerical diffusion is formed as a result of energy dissipation effects. It has also been noted in the literature that numerical diffusion can be used to model the effects of turbulence, which improves the convergence and stability of the mathematical calculation [5-10].

The principle of summarization of features, proposed in the study [11], is used to determine the flow around profiles when vortices and sources are distributed over the surface of load-bearing elements. Here it is applied to the three-dimensional case.

A prototype of a wind turbine with a vertical axis has been developed in the Laboratory of Mechanics of Fluid, Gas and Hydraulic Drive Systems of the Institute of Mechanics and Seismicity of the Academy of Sciences of the Republic of Uzbekistan. This sample can operate at low wind speeds and can be installed throughout the republic where there is sufficient wind potential.

This paper presents simulation results for a basic vertical axis wind turbine calculated using the commercial finite volume code Star-CCM+. Emphasis was placed on the dynamic characteristics of stall and wake formation, which have the greatest impact on turbine performance. A model is developed to reproduce the blade-wake interaction characteristic of higher tip speeds, which significantly improves the accuracy of the blade-element momentum model.

To numerically solve the system of initial nonstationary equations and the turbulence model $k-\varepsilon$. The finite element method and standard COMSOL Multiphysics 6.1 solvers were used.

Some results of calculating the flow around a rectangular airfoil at Reynolds numbers 10 000 $<Re<$ 2 000 0000 and angle of attack $\alpha = 0°–20°$ are presented. Speed results for different angle values showed that the implementation of the Comsol software package Multiphysics provides good convergence, stability and high accuracy of the model.

PHYSICO-MATHEMATICAL FORMULATION OF THE PROBLEM

The flow of a two-dimensional turbulent air flow around a rectangular profile is considered. The physical picture of the flow under study and the configuration of the calculated fields are shown in Fig.1.

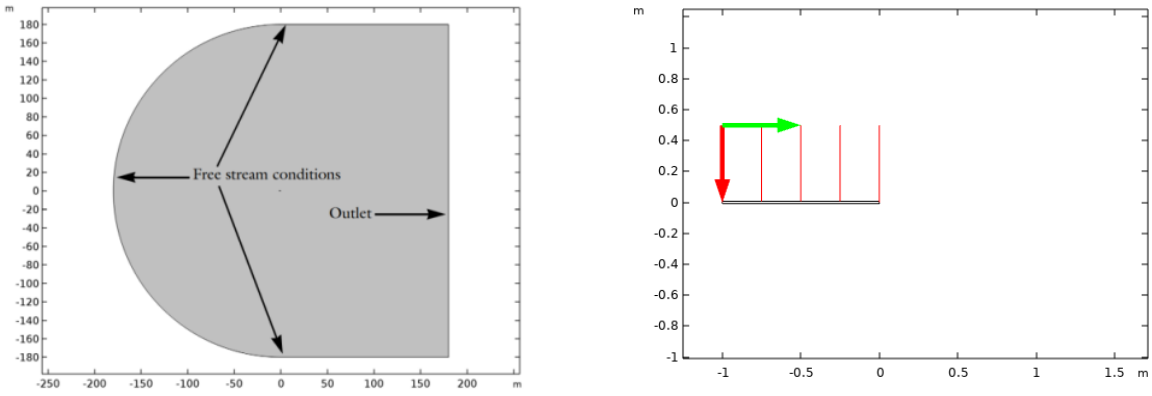

(a) (b)

FIGURE 1. Scheme of calculation areas. (a) profile flow (b) profile geometry

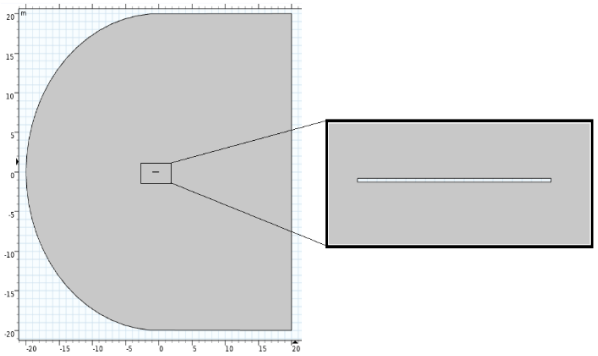

FIGURE 2. Flow profile geometry

For the flow problem around a rectangular airfoil, the Reynolds number based on the chord length is 10000<Re<2*10 ^{6}. Chord length c= 1 *m*. Options for the angle of attack of the profile from $\alpha = 0^0$ to $\alpha = 20^0$.

Numerical modeling takes into account the following laws of conservation and transfer of substances.

Equation of conservation of mass. This is the continuity equation, also called the general mass conservation equation [10-15]:

$$\frac{d\rho}{dt} + \nabla(\rho\vec{v}) = 0 \quad . \tag{1}$$

where ρ is the density of the liquid; $\vec{V}$ – velocity vector.

Equation of conservation of momentum. The general equation can be represented as follows [15-20]:

$$\frac{d}{dt}(\rho\vec{v}) + \nabla(\rho\vec{v}) = -\nabla_p + \nabla\overline{\overline{T}} + \rho g + F \,, \tag{2}$$

where p – static pressure; g and F are the gravitational force of the body and the external forces of the body, such as the influence of the dispersed phase, respectively.

The stress tensor $\overline{\overline{\tau}}$ is taken in the following form:

$$\overline{\overline{\tau}} = \mu\left[\left(\nabla\vec{v} + \nabla\vec{v}T - \frac{2}{3}\nabla\vec{v}I\right)\right], \tag{3}$$

here μ is molecular viscosity; I is the unit tensor.

Laminar flows are characterized by low Reynolds numbers. The higher the Reynolds number, the more likely the flow is to be turbulent. The Reynolds number gives a measure of the relative importance of inertial and viscous forces: for a wing it is defined as:

$$\mathrm{Re} = \frac{\rho u l}{\mu} \tag{4}$$

To find out whether the flow is laminar or turbulent, we need to calculate the Reynolds number:

$$\mathrm{Re} = \frac{\rho u l}{\mu} = \frac{1.2043*20*1}{1.81397*10^{-5}} = 1.327805*10^{6} \tag{5}$$

As can be seen from this large *Re* value, a developed turbulent flow regime is expected. Therefore, we should select a turbulent model that represents this process and use it to formulate and solve this problem.

Effect of flow turbulence. The presence of walls is critical to the specificity of turbulent flows. Obviously, the average velocity field is affected by the non-slip condition, which must be satisfied on the wall.

Viscous damping very close to the wall reduces tangential velocity, and kinematic locking reduces normal vibrations. However, the kinetic energy of turbulence caused by large mean velocity gradients rapidly increases turbulence towards the outer part of the near-surface region [14]. RSM and LES models $k-\varepsilon$ are best valid for turbulent core flows. Thus, it is necessary to think about how to make these models suitable for wall flows. Models Spalart and Almaras and $k-\varepsilon$ were designed for use throughout the entire boundary layer if the grid resolution is sufficient. This simulation experiment used a turbulent model $k-\varepsilon$ with standard wall function.

This choice is due to the possibility of a close-wall grating of the generated mesh. Turbulence model $k-\varepsilon$ is one of the most common options. This is a two equation model; It uses two additional transport equations to represent the turbulent properties of fluid flows. However, the SST model $k-\omega$ was also used in a simulation which did not produce realistic results and was therefore not consistent with the current model.

Modified model k - ε. Unlike well-known works, here it is proposed to use a modified $k-\varepsilon$ model:

$$\begin{cases} \dfrac{\partial}{\partial t}(\rho k)+\dfrac{\partial}{\partial x_j}(\rho k u_j)=\dfrac{\partial}{\partial x_j}\left[\left(\mu+\dfrac{\mu_t}{\sigma_k}\right)\dfrac{\partial k}{\partial x_j}\right]+G_k+G_b-\rho\varepsilon-2\rho\varepsilon M_t^2+S_k \\ \dfrac{\partial}{\partial t}(\rho\varepsilon)+\dfrac{\partial}{\partial x_j}(\rho\varepsilon u_j)=\dfrac{\partial}{\partial x_j}\left[\left(\mu+\dfrac{\mu_t}{\sigma_\varepsilon}\right)\dfrac{\partial\varepsilon}{\partial x_j}\right]+\rho C_1 S\varepsilon-\rho C_2\dfrac{\varepsilon^2}{k+\sqrt{\nu\varepsilon}}+C_{1\varepsilon}\dfrac{\varepsilon}{k}C_{3\varepsilon}G_b+S\varepsilon \end{cases} \quad (6)$$

which contributes to a more adequate description of heat and mass transfer processes. The notation used here are:

$$C_1=\max\left[0.43,\frac{\eta}{\eta+5}\right],\eta=S\frac{k}{\varepsilon},\ S=\sqrt{2S_{ij}S_{ij}},\ \mu_t=\rho C_\mu\frac{k^2}{\varepsilon},C_\mu=\frac{1}{A_0+A_S\dfrac{kU^*}{\varepsilon}},U^*=\sqrt{S_{ij}S_{ij}+\tilde{\Omega}_{ij}\tilde{\Omega}_{ij}},$$

$$\Omega_{ij}=\overline{\Omega}_{ij}-2\varepsilon_{ijk}\omega_k,\ A_S=\sqrt{6}\cos\varphi,\ \varphi=\frac{1}{3}\cos^{-1}(\sqrt{6}W),\ W=\frac{S_{ij}S_{jk}S_{ki}}{\tilde{S}^3},\ \tilde{S}=\sqrt{S_{ij}S_{ij}},S_{ij}=\frac{1}{2}\left(\frac{\partial u_j}{\partial x_i}+\frac{\partial u_i}{\partial x_j}\right),$$

$$G_k=-\rho\overline{u_i'u_j'}\frac{\partial u_j}{\partial u_i},\ S\equiv\sqrt{2S_{ij}S_{ij}},G_b=\beta g_i\frac{\mu_t\partial T}{\mathrm{Pr}_t\partial x_i},\ a_0=1/\mathrm{Pr}=k/\mu c_p,\beta=-\frac{1}{\rho}\left(\frac{\partial\rho}{\partial T}\right),\ G_b=-g_i\frac{\mu_t}{\rho\mathrm{Pr}_t}\frac{\partial\rho}{\partial x_i},$$

$$a=\sqrt{\gamma RT},\ \mathrm{Pr}_t=1/a_t,\ M_t=\sqrt{\frac{k}{a^2}}.$$

The empirical constants $k-\varepsilon$ of the model take standard values: $C_{1\varepsilon}=1.44$, $C_2=1.9$, $\sigma_k=1.0$, $\sigma_\varepsilon=1.2$, $A_0=4.04$. $k-\varepsilon$ the model appears to be the best model of first-level closure turbulence. For the turbulent energy mass density k, a system of two nonlinear diffusion equations is used to explain its turbulent quantities and turbulent energy dissipation rates ε. More than 30 years ago, a simpler version of this model appeared [14]. Since then, the model $k-\varepsilon$ has been widely used to calculate a wide range of problems, mainly to describe shear incompressible turbulence.

Calculation grids. In this work, a thickening of the mesh was used near the surface of the profile shown in Fig.3

For the area of flow around the profile, a computational mesh with 60200 elements was used. For the system of equations (1)-(3), obvious boundary conditions for adhesion on solid walls are specified. The output accepts extrapolation conditions for all parameters. At the inlet, uniform profiles of the longitudinal velocity component c were applied $V_x=U_0$, the transverse velocity component and pressure were assumed to be zero $V_y=P=0$. Also at the input are the values of relative velocities (disturbances): $v_x=0.004$, $v_y=0$.

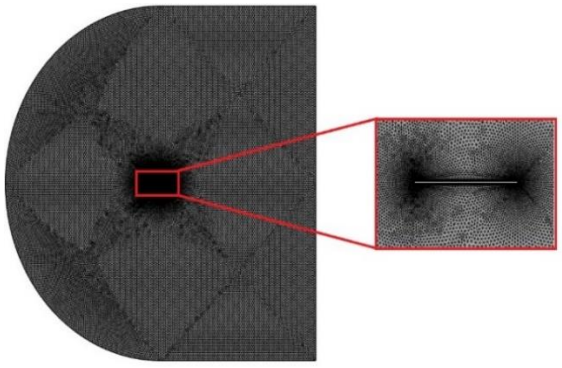

FIGURE 3. Calculation mesh of flow around the profile

The dimensions of the initial data for calculating the dimensional parameters were taken as follows: wind speed – m/s, angular speed – rad/s, air density – kg/m^3 (Fig. 4).

Label: Parameters 1

Parameters

Name	Expression	Value	Description
U_inf	20[m*s^-1]	20 m/s	Free-stream velocity
rho_inf	1.2043[kg*m^-3]	1.2043 kg/m³	Free-stream density
mu_inf	1.81397e-5[kg*m^-1*s^-1]	1.814E-5 kg/(...	Free-stream dynamic vis...
L	20[m]	20 m	Domain reference length
c	1[m]	1 m	Chord length
k_inf	0.1*mu_inf*U_inf/(rho_inf*L)	1.5062E-6 m²/s²	Free-stream turbulent kin...
om_inf	10*U_inf/L	10 1/s	Free-stream specific dissi...
alpha	0	0	Angle of attack
Re	U_inf*c*rho_inf/mu_inf	1.3278E6	

FIGURE 4. Source data window with dimensions and values

SOLUTION METHOD AND RESULTS

Time-averaged and longitudinal velocity (or flow velocity) profiles allow the flow characteristics to be assessed at various points downstream of the profile. Time-averaged and normalized longitudinal velocity profiles are evaluated at five points (x/c = 0, 0.25, 0.5, 0.75, and 1) behind the profile.

In Fig. Figure 5 shows graphs of longitudinal velocity in various sections at angle of attack values $\alpha = 2^0, 6^0, 10^0, 14^0, 18^0, 20^0$. The speed of the undisturbed flow was 20 m/s, and the Reynolds number was 1,327,800.

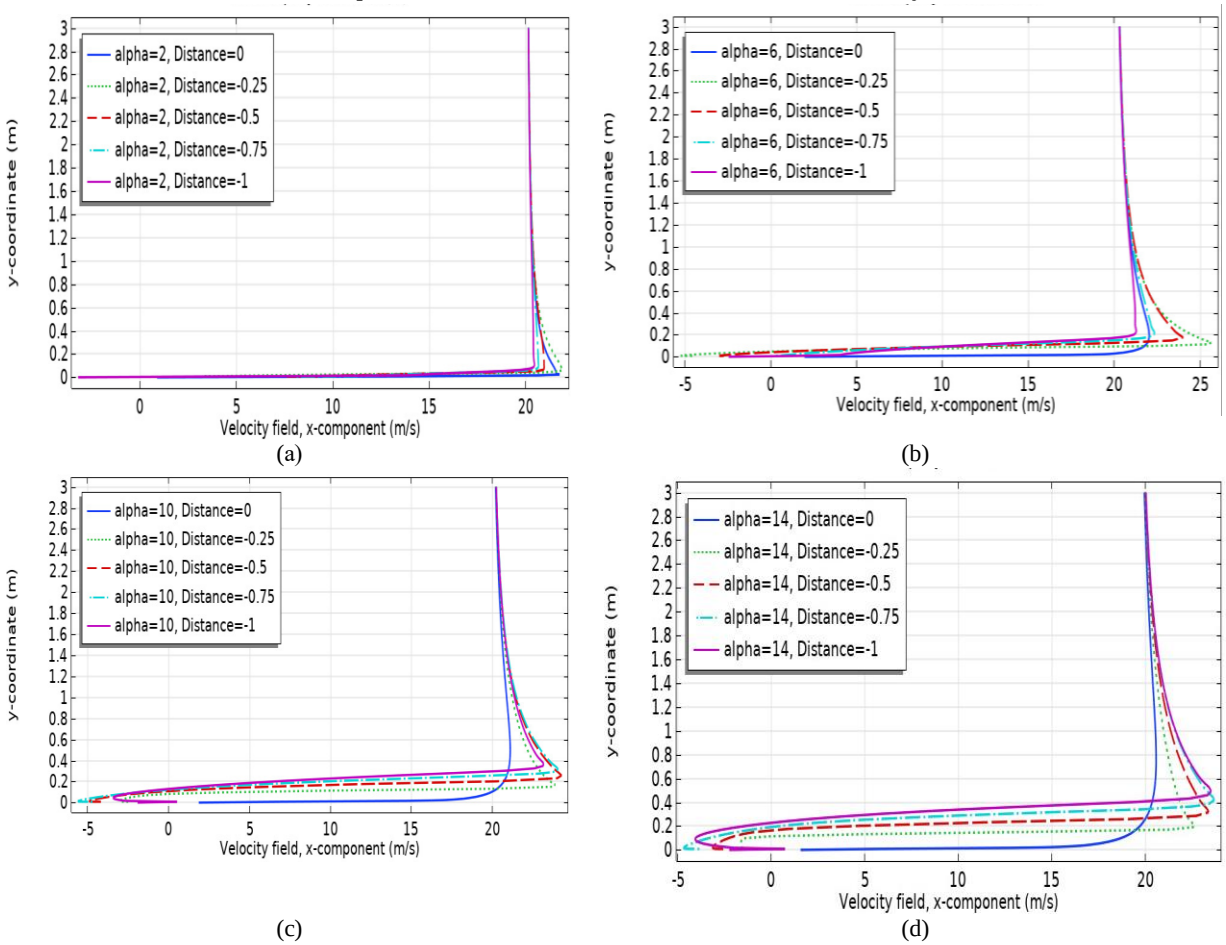

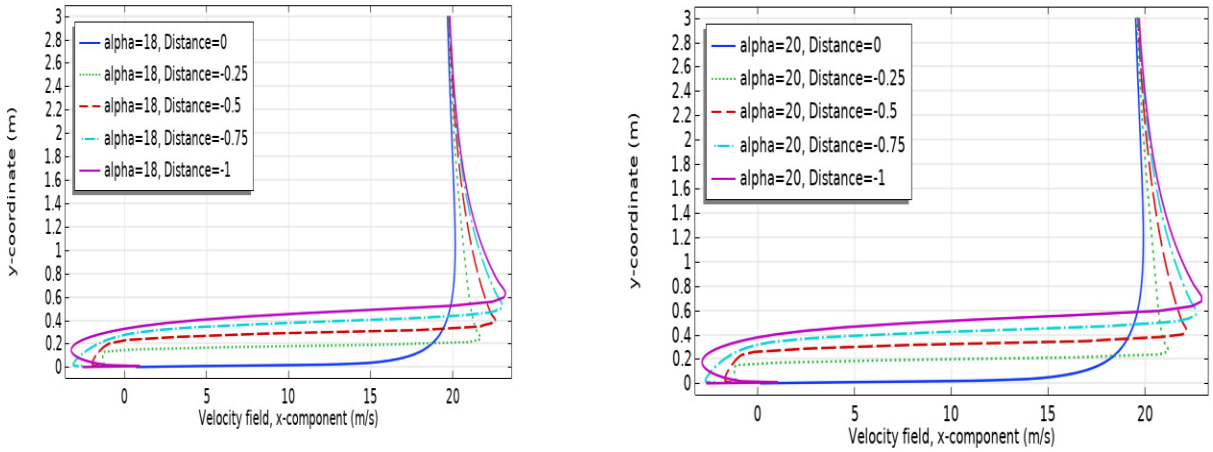

(e) (f)

FIGURE 5. Longitudinal velocity field at sections *x/c* = 0, 0.25, 0.5, 0.75,1 at (a) alpha=2, (b) alpha=6, (c) alpha=10, (d) alpha=14, (e) alpha=18, (f) alpha=20

At the angle of attack of the wing, $\alpha=2^0$ the highest longitudinal speed of *22.1 m/s* is observed at *x/c =0.25*, and the lowest speed is at *x/c =1*. With this installation of the wing, it is clear that high speed is generated on the opposite side of the slope and in the initial part of the plate. As the plate moves upward, the influence of the plate weakens and the flow again acquires its initial speed. The change in speed along the axis y is not that great, i.e. the results did not differ much from the results of flow around a plate at an angle $\alpha=0$, since in this case the angle of attack of the wing is not large.

The highest flow rate at $\alpha=6^0$ also has at point at $x/c=0{,}25$. When $x/c=1.00$ he reached a low speed. In this case, the maximum speed was 25.07 m/s. At this angle of attack of the wing, the flow velocity at the point $x/c=0{,}5$ equal to 23.8 *m/s*. After *y=1 m*, the results of the stream took on the same value as in the original stream.

Maximum speed at a point $x/c=0{,}5$ near the wing at $\alpha=10^0$ was *22.9 m/s*. At points $x/c=0{,}25$ And $x/c=0{,}75$ the longitudinal velocity took on almost the same value. There is a noticeable tendency that the highest velocity values in the sections move upward in height and in this case, after *y=1,5 m*, the results of the longitudinal velocity tend to their undisturbed value. It has been found that this angle of attack value produces the desired torque results to drive the rotational motion of the wing at this distance.

When the angle of attack of the wing $\alpha=14^0$ is at the point $x/c=0{,}75$ the maximum speed observed was *23.2 m/s*. At points $x/c=0{,}5$. And $x/c=1{,}0$ the speed took on almost the same value. At the point $x/c=0$ it reaches low speed. After height *y=1,85 m* longitudinal velocity is practically not disturbed. And in this case there is a favorable opportunity for wing rotation.

The tendency for the highest velocity value to shift upward in height at the angle of attack $\alpha=18^0$ reaches its completion: the maximum speed of *23.2 m/s* is achieved at the end point $x/c=1{,}0$, i.e. at the end of the wing. At the same time, at points $x/c=0{,}75$ and $x/c=0{,}5$ the speed took on almost equal values. As the angle of attack increases, the size of the generated vortex increases. Calculations up to a height of 3 meters showed that in this case, after *y=2,2 m* disturbances in the longitudinal flow velocity are not significant.

At the angle of attack of the wing $\alpha=20^0$, the maximum speed equal to *23.8 m/s* is observed at the end of the wing (i.e. at $x/c=1{,}0$). At the point $x/c=0{,}75$ the speed has a value of *23.5 m/s*. At a point $x/c=0$ (at the beginning of the wing) it reached a small value. As the angle of attack increases, you can also see an increase in drag. Results at 3 m downstream of the wing were analyzed as this is the critical span for wing performance.

CONCLUSION

At different angles of attack, longitudinal velocity fields were obtained and analyzed in a two-dimensional setting. Modeling of wall friction stresses can be reliable if the boundary layer characteristics are defined correctly. An erroneous determination of the boundary layer characteristics can lead to a distortion of the pressure coefficient corresponding to the aerodynamic force factors.

ACKNOWLEDGMENTS

The research was conducted at the expense of basic budget funding from the Academy of Sciences of the Republic of Uzbekistan.

REFERENCES

1. P. A. Kozak, David Vallverdú and Dietmar Rempfer, Journal of Propulsion and Power **32(3)**, 592-601 (2016).
2. R. A. Fayziev, and F. M. Kurbanov, *VI International Scientific Forum on Computer and Energy Sciences*, E3S Web of Conferences, edited by D. Bazarov (EDP Sciences, Tashkent, 2022), 020015
3. R. Lanzafame, S. Mauro and M. Messina Energy Procedia **45**, 131 (2014)
4. P. R. Ashill, AGARD **335**, 85-88 (1993).
5. E. M. Murman, AIAA Paper **72(1007)**, 45403 (2015).
6. A. E. P. Veldman, AIAA Journal **19(1)**, 79-85 (198l).
7. J. Winslow, H. Otsuka, B. Govindarajan and I. Chopra, Journal of Aircraft **61(3)**, 104-110 (2017).
8. P. B. S. Lissaman, Annual Reviews of Fluid Mechanics **15**, 12-43 (2019).
9. J. G. Leishman *Principles of Helicopter Aerodynamics* (Cambridge University Press, Cambridge, 2006), pp.12-15.
10. R. Kojima, T. Nonomura, A. Oyama and K. Fujii Large-Eddy, Journal of Aircraft **50(1)**, 187–196 (2013).
11. S. P. Sane, Journal of Experimental Biology **206(23)**, 4191–4208 (2013).
12. M. Edwards, L. Angelo Danao and R.J. Howell, Journal of Solar Energy Engineering **134(3)**, 11-14 (2012).
13. S. Velichko and Yu. B. Lifshitz, Theor Comput Fluid Dynamics **7(3)**, 189-206 (1995).
14. I. Khujaev, O. Toirov, J. Jumayev and M. M. Hamdamov "Modeling of vertical axis wind turbine using Ansys Fluent package program",in *V International Scientific Conference "Construction Mechanics, Hydraulics and Water Resources Engineering"*, E3S Web of Conferences, edited by D. Bazarov (EDP Sciences, Tashkent, 2023), 04040.
15. M. M. Hamdamov "Numerical modeling of wind turbine with vertical axis using turbulence model $k-\omega$ in Ansys Fluent", in *V International Scientific Conference "Construction Mechanics, Hydraulics and Water Resources Engineering"*, E3S Web of Conferences, edited by D. Bazarov (EDP Sciences, Tashkent, 2023), 02024.
16. K. Pope, I. Dincer, and G.F. Naterer, Renewable Energy **35(9)**, 2102–2113 (2010).
17. P. Gulve and Sh. Bh. Barve, International Journal of Mechanical Engineering and Technology (IJMET) **5(10)**, 148–155 (2014).
18. F. Balduzzi, J. Drofelnik, A. Bianchini, G. Ferrara, L. Ferrari and M.S. Campobasso, Energy **128**, 550 (2017).
19. H. F. Lam and H. Y. Peng, Reneweable Energy **90(C)**, 386–398 (2016).
20. R.Lanzafame, S.Mauro and M.Messina, Energy Procedia **45(7)** 131-140 (2014).